

Tomographic Imaging with Cosmic Ray Muons*

C. L. Morris,¹ C. C. Alexander,¹ J. D. Bacon,¹ K. N. Borozdin,¹
D. J. Clark,¹ R. Chartrand,¹ C. J. Espinoza,¹ A. M. Fraser,¹
M. C. Galassi,¹ J. A. Green,¹ J. S. Gonzales,¹ J. J. Gomez,¹
N. W. Hengartner,¹ G. E. Hogan,¹ A. V. Klimenko,¹
M. F. Makela, P. McGaughey¹, J. J. Medina,¹
F. E. Pazuchanics,¹ W. C. Priedhorsky,¹ J. C. Ramsey,¹
A. Saunders,¹ R. C. Schirato,¹ L. J. Schultz,¹ M. J. Sossong,¹
and G. S. Blanpied²

¹Los Alamos National Laboratory, Los Alamos, NM, USA

²University of South Carolina, Columbia, SC, USA

Over 120 million vehicles enter the United States each year. Many are capable of transporting hidden nuclear weapons or nuclear material. Currently deployed X-ray radiography systems are limited because they cannot be used on occupied vehicles and the energy and dose are too low to penetrate many cargos. We present a new technique that overcomes these limitations by obtaining tomographic images using the multiple scattering of cosmic radiation as it transits each vehicle. When coupled with passive radiation detection, muon interrogation could contribute to safe and robust border protection against nuclear devices or material in occupied vehicles and containers.

INTRODUCTION

One of the strategies to make weapons of mass destruction (WMD) unavailable to terrorists is by controlling nuclear material at its source. An additional reduction in risk can be obtained by increasing the likelihood of detection of

*LA-UR-07-3100, Los Alamos National Laboratory.

Current address for A. V. Klimenko, Passport Systems, Inc., 15 Craig Road, Acton, MA 01720.

Received 27 June 2007; accepted 17 March 2008.

This work has been partially supported by LDRD, NA-22 of the DOE, DARPA, DNDO, and Decision Sciences Corporation. The views and conclusions contained in this material are those of the authors and should not be interpreted as necessarily representing the official policies, either expressed or implied, of the sponsors.

Address correspondence to Chris Morris, Los Alamos National Laboratory, Los Alamos, Group P-25, Mailstop H846, NM 87544, USA. E-mail: cmorris@pobox1663.lanl.gov

illicit transport of these materials at transportation checkpoints, such as border crossings.¹ Customs agencies around the world have begun using a set of radiation detectors and X-ray scanners at border crossing for this purpose.² However, passive counting does not provide robust detection of hidden special nuclear material (SNM) because all of the signals can be obscured combining a relatively small amount of material having high atomic number (Z), such as lead tungsten, with hydrogenous (polyethylene) and neutron-absorbing (lithium or boron) shielding. More sophisticated counting techniques, such as directional gamma and neutron counting, and better energy resolution may improve the sensitivity and limit some options for hiding SNM. However, because of practical counting time limits and natural background rates, well-shielded material can be moved through the best possible passive systems.

Photon (X-ray or gamma-ray) radiography provides a method of examining cargo and transport vehicles for the presence of hidden material. Penetration and scatter background limit the utility of this technique.³ New scanning photon radiography machines in combination with neutron scatter and radiography and X-ray back-scatter might provide an approach for detecting shielded, hidden SNM. The potential doses to vehicle occupants and to operators limit this technology option to examining only a small fraction of cross-border traffic.

MUON TOMOGRAPHY

Here we present results from a study of a new technique that is capable of passively detecting shielded SNM in a short time by using the multiple scattering of cosmic ray muons as a radiographic probe.⁴ This technique is selective to high- Z materials, both SNM and high- Z shielding materials.

The trajectory of a charge particle through any material is the result of the convolution of many small deflections due to Coulomb scattering from the charge of the atomic nuclei in the medium. The net angular and position deflection of the trajectory are very sensitive to the charge (Z) of the atomic nuclei. High-energy particles are more strongly affected by materials that make good gamma-ray shielding and by SNM than by the materials that make up normal cargo such as people, paper, aluminum, and steel.

The earth is continuously bombarded by energetic stable particles, mostly protons. These interact in the upper atmosphere through the nuclear force, producing showers of particles that include many short-lived particles called "pions." The pions decay, producing muons. Muons interact with matter primarily through the Coulomb force and have no nuclear interaction. The Coulomb force removes energy from the muons more slowly than nuclear interactions. Consequently, many of the muons arrive at the earth's surface as penetrating, weakly interacting charged radiation. The flux at sea level is about 1 muon/cm²/min in an energy and angular range useful for tomography.⁵

Conventional radiography takes advantage of the absorption of penetrating radiation. For X-ray radiography,⁶ the areal density of the object seen in a pixel of the image is determined by the absorption or scattering of the incident beam: $N = N_0 e^{-L/L_0}$,⁷ where L is the path length (areal density) through an object, and L_0 is the mean free path for scattering or absorption. The precision of radiographic measurements is limited by the Poisson counting statistics of the transmitted flux, $\frac{\Delta L}{L_0} = \frac{1}{\sqrt{N}}$. The maximum mean free path for photons in high-Z elements occurs at a few MeV. The mean free path is approximately 25 g/cm² for all materials at this energy. This corresponds to less than 2 cm of lead. Penetrating objects of tens of L_0 requires very large incident doses.

An alternative to the absorption signal is the multiple Coulomb scattering signal.^{8,9} The many small interactions add up to yield an angular deviation that follows a Gaussian distribution to a good approximation: $\frac{dN}{d\theta_x} = \frac{1}{\sqrt{2\pi}\theta_0} e^{-\theta_x^2/2\theta_0^2}$.¹⁰ The width of the distribution is related to the scattering material: $\theta_0 = 14/p\beta\sqrt{L/X}$, where p is the particle momentum, β is the velocity divided by the velocity of light, and X is the radiation length. Here we have dropped logarithmic terms that are on the order of 10%. In a layer 10 cm thick, a 3-GeV muon will scatter with a mean angle of 2.3 mrad in water ($X = 36$ cm), 11 mrad in iron ($X = 1.76$ cm), and 20 mrad in tungsten ($X = 0.56$ cm). If the muon scattering angle in an object can be measured, and its momentum is known, then the path length, $\Delta l/l$ can be determined to a precision of $\frac{\Delta l}{l} = \sqrt{2/N}$, where N , the number of transmitted muons, is very nearly equal to the number incident. Thus, each transmitted muon provides information about the thickness of the object.

Muon momentum information can be obtained inexpensively by measuring the multiple scattering resulting from several layers of scatterer of known thickness. These scatterers can be the detectors themselves if multiple layers are used. The precision of momentum determination is approximately given by $\frac{\Delta p}{p} = \frac{1}{\sqrt{2N_p}}$, where N_p is the number of scattering layers (the factor of two arises because x and y are measured independently). Even with just two planes, one obtains $\frac{\Delta p}{p} = 0.5$ which is adequate for a first-order momentum correction.

The flux of muons through a 10-cm cube of material in 60 s is sufficient to measure its thickness in radiation lengths to a precision of 14%. With these statistics a cube of tungsten can be distinguished from a cube of steel at the six standard deviation level.

We have demonstrated a suitable detector technology, drift tubes, and developed tracking algorithms in a medium-scale experiment. Here we report the results of this work. Additionally, we have used the GEANT Monte Carlo Transport program to validate reconstruction and detection algorithms for muon tomography for border security applications.

EXPERIMENTAL DEMONSTRATION

We have constructed a large muon tracker (LMT) consisting of 12 planes of 0.05-m-diameter, 3.65-m-long drift tubes configured with three crossed $x - y$ sets of detectors both above and below a sample volume. A photograph of the LMT is shown in Figure 1. A complete description of the apparatus is given elsewhere.¹²

Signals from the detectors were amplified and discriminated with a commercial comparator board and were digitized with Versa Module Europa (VME) time to digital converters (CAEN[®] 767B) and read into a computer using PC DAQ.¹³ The detectors measured position to a precision of about 400 μm full width at half maximum (FWHM) and angles to about 2 mrad FWHM. These include the instrumental contributions from multiple scattering in the detectors, intrinsic detector resolution, and residual alignment errors.

The LMT has some limitations. A robust tracker that fits time zero and eliminates the need for a fast trigger has recently been implemented, increasing the solid angle significantly. However, the counting rates are a factor of four to five below those that would be obtained in a four-sided scanner because the detector has a limited solid angle of less than one steradian.

Despite limitations, the LMT has provided an important test bed that has been used to develop our techniques and algorithms and that has been used to

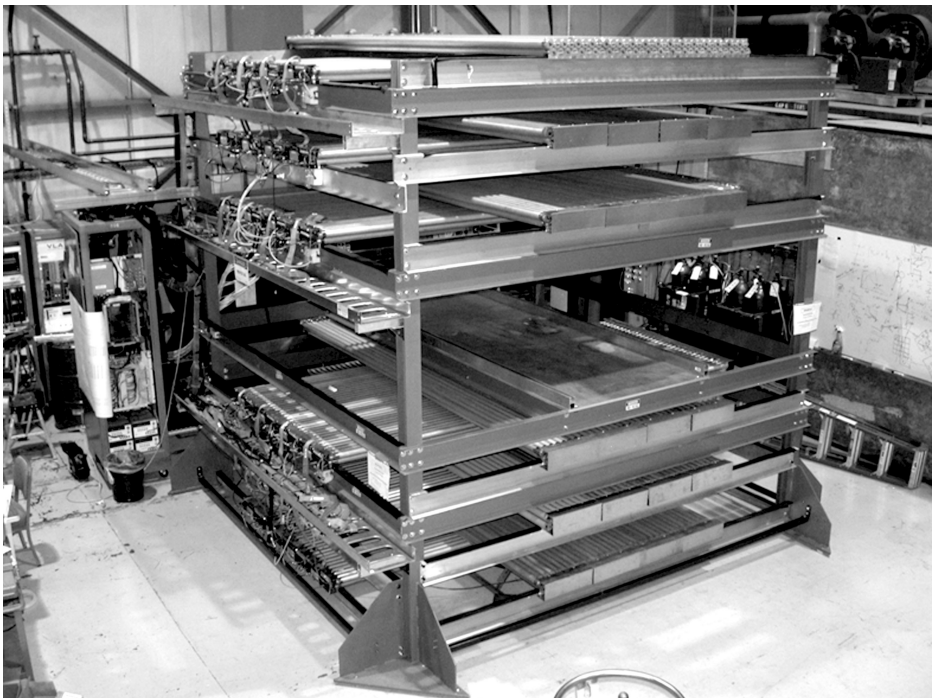


Figure 1: The experimental apparatus.

validate the cosmic ray model used in Monte Carlo simulations. Two very important accomplishments from the work with the LMT have been the development and demonstration of automatic calibration of the drift tube positions and drift time to position look up tubes using cosmic rays and a time zero fitter that eliminates the need for a prompt trigger for obtaining tracking information.

The data were processed with a simple reconstruction technique. The $1.5 \times 1.5 \times 1.0 \text{ m}^3$ sample volume was segmented into $2 \times 2 \times 2 \text{ cm}^3$ voxels. The median scattering angle was calculated for all muons with entering and exiting trajectories that intersect a voxel within an adjustable distance, d . This distance was set to the size of a threat object (5 cm) for the receiver operator characteristic (ROC) work presented below. For imaging, it was set to the voxel size. Because of the limited solid angle of the LMT, tomographic reconstructions suffer from considerable vertical blur, are noisy, and have not been used in this study.

A study of how quickly a nuclear threat object can be identified has been performed using a $10 \times 10 \times 10 \text{ cm}^3$ cube of lead to represent the threat. This was mounted in the LMT along with an automobile engine and transmission. A photograph of the set up is shown in Figure 2.

Approximately 160 min of data have been analyzed to obtain the images shown in Figure 3. The mean scattering angle for all trajectories that pass



Figure 2: Photographs of the engine in the LMT.

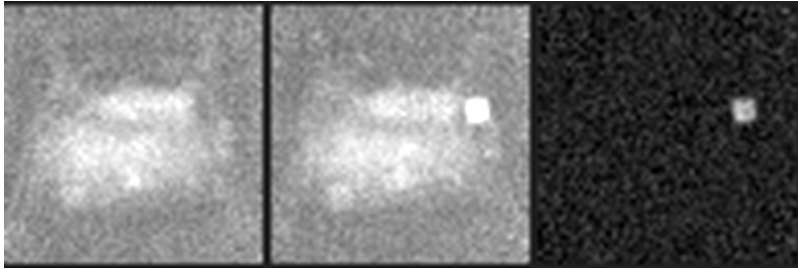


Figure 3: Mean scattering angle for a slice through the scene 50 cm above the base plate. The left panel shows the engine, the middle panel the engine plus the $10 \times 10 \times 10 \text{ cm}^3$ lead sample, and the right panel the difference.

through each voxel is plotted. In spite of the simplicity of this analysis, the lead stands out dramatically.

We have broken the data set into 1-, 2-, and 4-min intervals and analyzed each independently. The average picture from the long run with only the engine was subtracted from each of the individual short runs, and the maximum $10 \times 10 \times 10 \text{ cm}^3$ voxel value was histogrammed for all of the runs with and without the lead. These histograms (an example is shown in Figure 4) were used to calculate the ROC curves, shown in Figure 5.

From the ROC curves shown above it is apparent that the lead objects can be identified perfectly (given that 40 trials were used) with zero false identifications in 4 min. When scaled to sea level muon fluxes and full solid angle these times can be divided by 5. Fifty percent knowledge of momentum, which modeling shows can be obtained by analyzing position residuals from the tracking, is expected to reduce counting times by another factor of 1.5–2.

It is important to point out that these data were obtained using position calibrations for the tubes obtained using cosmic ray data and an automated

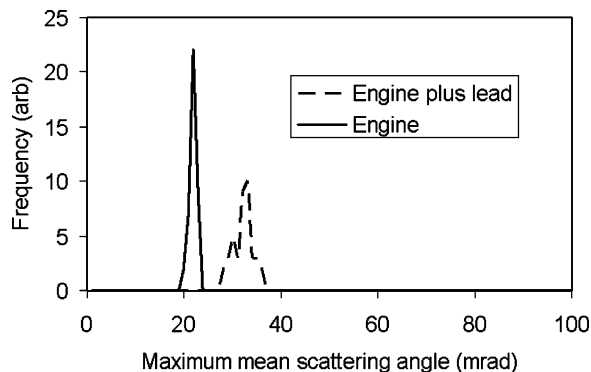


Figure 4: Histograms of the peak value of mean scattering angle, with a $10 \times 10 \times 10 \text{ cm}^3$ average applied to the $2 \times 2 \times 2 \text{ cm}^3$ voxels in a set of forty 4-min reconstructions with the engine in the LMT.

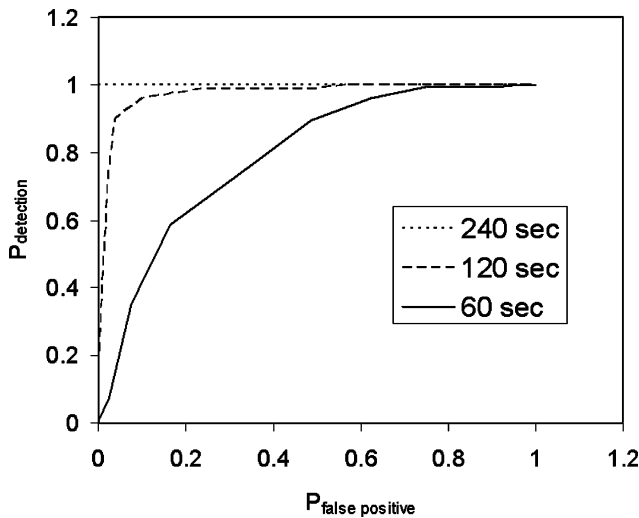


Figure 5: ROC curves for identifying the lead object mounted in the LMT with the engine.

calibration procedure that found the relative positions of each end of all of the tubes, and prompt time for the drift tubes was determined by fitting it as a parameter in the trajectory fits; i.e., there was no need for a timing scintillator.¹²

PASSIVE COUNTING

Currently, portal monitors and other radiation detectors are deployed at many sites to detect the surreptitious transport of nuclear materials. Although these detectors are quite effective at detecting radiation, innocuous alarms from a variety of radioactive cargo make their use cumbersome and the potential for shielding nuclear material allows for their defeat as a nuclear threat deterrent. The absence of a radiation signal does not eliminate the possibility of a nuclear threat. Muon tomography (MT) provides a method that is effective at detecting high-Z (atomic number) material in liter-sized volumes. The same detectors that are used to detect and track muons can be used to measure radiation from a nuclear device as well as to identify the presence of enough shielding to hide the nuclear signal.

Radiation dispersal devices (RDD) can be constructed using only grams of active material. Such small quantities can be easily hidden from any radiographic technique in an object the size of a passenger vehicle, truck, or cargo container. However, nearly all of the candidate materials for an RDD are either strong gamma ray or beta ray emitters. We have performed experiments that show that the radiation signature from the quantity of material needed to construct an effective RDD is enormous and is easily detectable even with several inches of high-Z shielding (lead).

The self-shielding produced by normal cargo tends to reduce the background counting rates in portal monitors by up to 10% when the cargo is present. This reduction can mask a radiation increase. This places a limit on how well excess radiation from cargo can be measured. MT provides an integral measure of the cargo measured in mass units weighted by radiation lengths. This may provide a good estimate of the self-shielding of natural background so that small signals can be detected.

There may be other signatures of nuclear weapons materials that are enabled by the large solid angle and high efficiency of the muon detectors. In addition to the gamma and X-ray signal, ^{238}U spontaneously fissions, producing neutrons. The large solid angle and high multiplicity of counters used for MT should provide for efficient neutron counting, if ^3He gas is added to the drift tubes and some moderating material is added to the walls. Five Kilograms of highly enriched uranium (HEU) emits about 5 neutrons per second from the 8% of ^{238}U .¹⁴ A distinctive feature of these neutrons is that they are emitted in correlated bursts with a mean multiplicity of 2.1.¹⁵ These neutrons can cause further fissions in surrounding material increasing the multiplicity.

Fusing neutron, neutron multiplicity, gamma ray and tomographic data from an MT scanner may provide a highly effective way to detect several kilogram quantities of HEU, considered the most challenging of nuclear material to find. Of course, larger quantities are distinctive in the tomography as well as in their neutron and gamma signals.

MONTE CARLO SIMULATIONS

In order to examine how well this technique works for complex objects we have used the Monte Carlo simulation package, GEANT¹¹ to generate cosmic-ray muons with the appropriate distribution of energies and angles, propagated them through a test volume, and generated the positions and angles at which they would be detected in a four-sided scanner. The muon spectrum, angular distribution, and rate were appropriate for sea level. We have studied a set of scenes for threat objects in a cargo van.

The cosmic-ray event generator used in the Monte Carlo studies was validated using data taken with the LMT. The validation included adjustment of the generator for the altitude of Los Alamos. In addition, the scattering angle distributions were reproduced by GEANT simulations. We did not use the 3-D reconstruction algorithm described below with the LMT data, because its limited solid angle made it difficult to localize scattering centers in the vertical coordinate.

We have modeled the following scenes:

1. An empty van.
2. A $4' \times 8' \times 3'$ high stack of boron treated plywood with or without an object of interest (OOI) inside. The total weight of the plywood is about 1800 kg.

3. A welding machine. Two 0.75-in steel plates, top and bottom, are included in order to try to spoof the reconstruction technique.
4. A box of clutter. Reduced-density concrete powder (0.5 g/cm^3) is filled with randomly placed objects of four different shapes: half of a sphere, rectangular block of two different sizes, and a parallelepiped. Each individual piece of clutter is randomly placed, rotated, and offset with respect to the center of the given piece of clutter. The material for each of the pieces is randomly assigned to be various clutter material such as plastic, glass, and steel. The total weight of the scene is approximately 3200 kg.

A visualization of the model for each of these scenes is shown in Figure 6. Each scene was modeled with and without a 10-cm cube of tungsten hidden in the cargo. The empty van was modeled with the tungsten under the engine and above the differential.

The borated plywood was chosen because it provides a considerable amount of moderating material and the boron quickly absorbs the moderated neutrons so it acts as a shield against active interrogation. Plywood alone increases the fission signal from active interrogation because the fission cross sections are much larger for moderated neutrons than for fast neutrons. The welding machine is clutter that radiographically looks like a common object. The box of clutter is intended to look like a box of complex junk. The special three-layer container is a composite shield in which nuclear material is hidden from passive counting with medium mass materials.

For reconstruction of these scenes we used a maximum likelihood-based tomographic algorithm. The foundations of this algorithm were developed in a Ph.D. dissertation in 2003.¹⁶ We developed a fast, robust implementation of this approach (MELM) with results described below.¹⁷

A composite of reconstructions of the three cargo scenes and two additional scenes of the empty van with a threat object located over the differential and under the engine, respectively, is shown in Figure 7. The nature of each of these scenes is clearly visible from the reconstructions. Automatic identification of

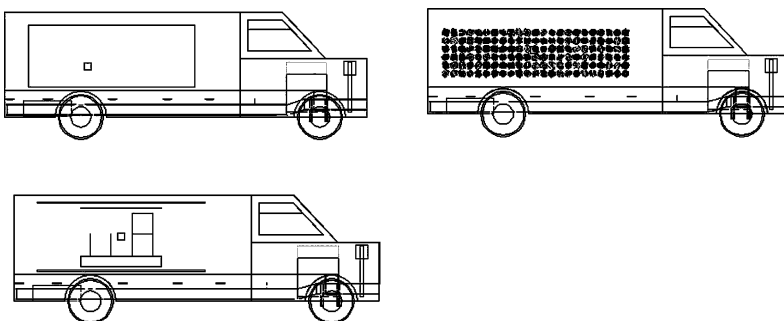


Figure 6: The four scenes that have been modeled are depicted here: a) 3-foot-high stack of 4×8 foot sheets of borated plywood; b) a box of clutter; c) a welding machine.

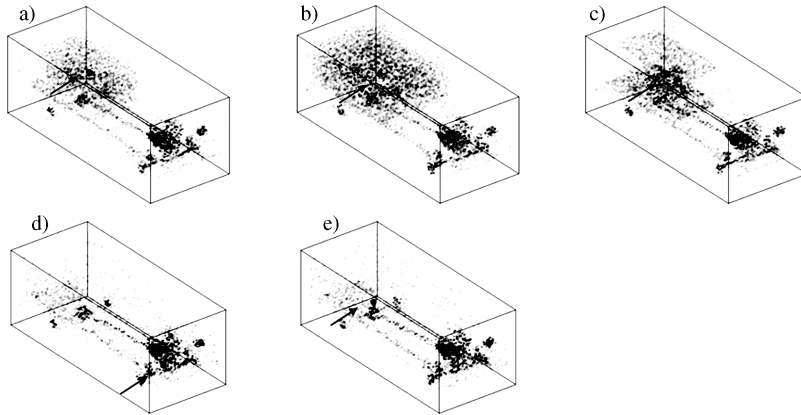


Figure 7: Reconstructions made from 1-min cosmic ray exposures for each of the scenes described above. The threat object is marked with an arrow in each of the reconstructions.

threat objects using a simple density threshold for 1000 cm^3 volumes is possible for all of these scenes.

Automatic identification of threat objects has been studied by calculating the average reconstructed scattering density for all possible 10-cm cubes from the 5-cm voxels. The maximum values of this quantity for 100 simulations and reconstructions performed for each of the five scenes shown above plus their empty counterpart for exposure times ranging from 15, 30, and 60 s are shown in Figure 8. As the exposure time increases, the threat objects become better separated from the innocuous cargo scenes.

The impact of momentum uncertainty has been estimated by adding Gaussian distributed uncertainty to the perfect momentum and then performing reconstructions and calculating ROC curves. The time needed to obtain similar ROC curves is increased by $\sim 50\%$ when 50% momentum knowledge (obtained from four residual measurements in the tracking detectors) rather than perfect knowledge is assumed. The robustness of the median reconstruction method reduced the statistical impact of imperfect momentum knowledge.

These reconstructions have been used to generate ROC curves. ROC curves show the relationship between the false positive rate *vs.* the detection rate for threat objects as the threshold is varied. The ROC curves indicate that innocent vehicles can be identified with as little as 15 s of counting time. By 90 s the identification is very good.

The analysis of the layered object and differences between the ROC curves for an object under the engine and above the differential has led to an improved technique for regularizing the reconstructions. We have found that heavily regularizing for longer exposures tends to reduce the signal from the threat objects when they are located near a feature such as the engine or inside of the iron box of the layered object. For short exposures, regularization is important

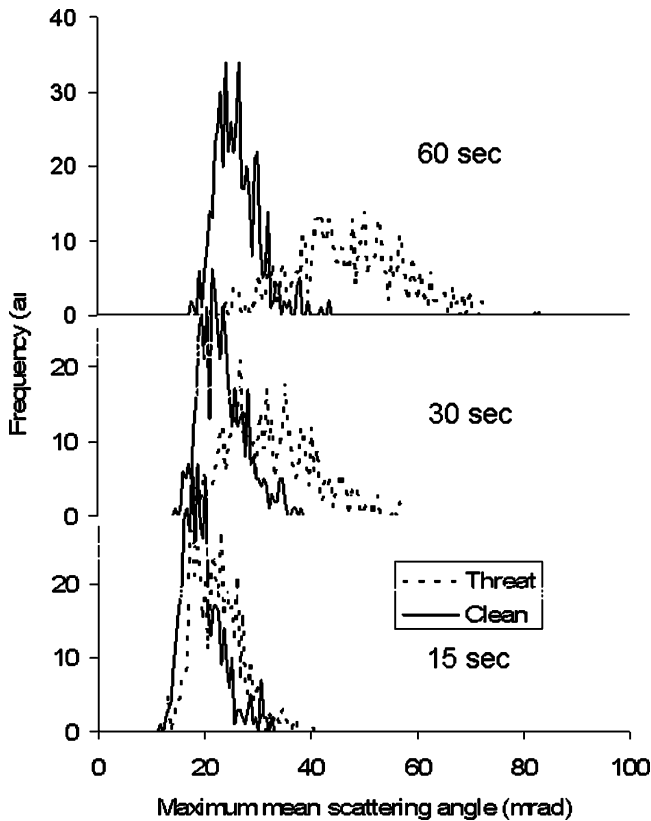


Figure 8: Histograms of the maximum value for the average reconstructed density in van scenes shown in Figure 7.

for reducing the noise in innocuous scenes in order to reduce the number of unresolved false positives. A technique that uses heavy regularization at short exposures and little or no regularization at late times has been found to give better results than fixed regularization. Using this method gives the ROC curves shown in Figure 9.

The use of prior knowledge considerably speeds up identification of threat objects. When prior knowledge was not assumed and 50% momentum knowledge was used, 90% detection with zero false positives on the data set used for these ROC curves requires ~ 60 -s counting times. When an average of many reconstructions of an empty van for a given time is used and subtracted from the cargo scenes the rate of false positives for short scanning times is significantly reduced. A deployed device would have equivalent information about common vehicle models in a data base. Histograms of the maximum reconstructed values obtained using three sigma subtraction (the average empty van reconstruction plus three times the standard deviation in a set of statistically independent reconstructions for a given scanning time is subtracted voxel by voxel) are shown

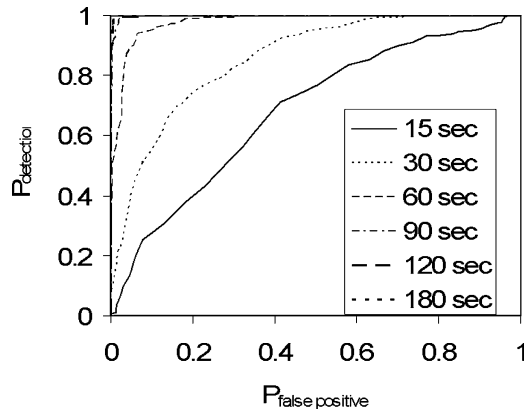


Figure 9: Eight voxel ROC curves for the set scenes shown above. These ROC curves have been generated using 1000 independent simulations at each of the time shown in the legend.

in Figure 10 and ROC curves are shown in Figure 11. With this procedure the 30-s ROC curve becomes nearly perfect. Plots of the required inspection times are shown in Figure 12.

The dashed curve shows the results that are obtained when the average of many empty van scenes is subtracted from each run before the ROC curve is calculated. This reduces the average level of the signal from the innocuous scenes and results in a factor of two reduction in average scanning time. Finally, the dot-dash curve has been obtained by subtracting the average signal plus three standard deviations (three sigmas) from the reconstruction at each time. This oversubtracts in regions of high density where statistical fluctuations leading to false positives are most likely. This method reduces inspection times by nearly an additional factor of two.

More work is needed to optimize inspection times for this latter method. There is clearly important information that could be obtained by using reconstructions at even shorter inspection times than the minimum 15 s studied here.

IMPLEMENTATION

A drawing illustrating how this idea might be implemented at a border crossing is shown in Figure 13. The walls of a scanning device are constructed from 12 layers of position-sensitive sealed drift tubes. Two layers offset by a tube radius are used for each coordinate measurement, and three measurements are made in each of two orthogonal planes for the incident trajectory and the same for the exit trajectory. This provides considerable redundancy to ensure robust particle tracking, as well as providing enough information so that the track residuals can be used for momentum estimation.

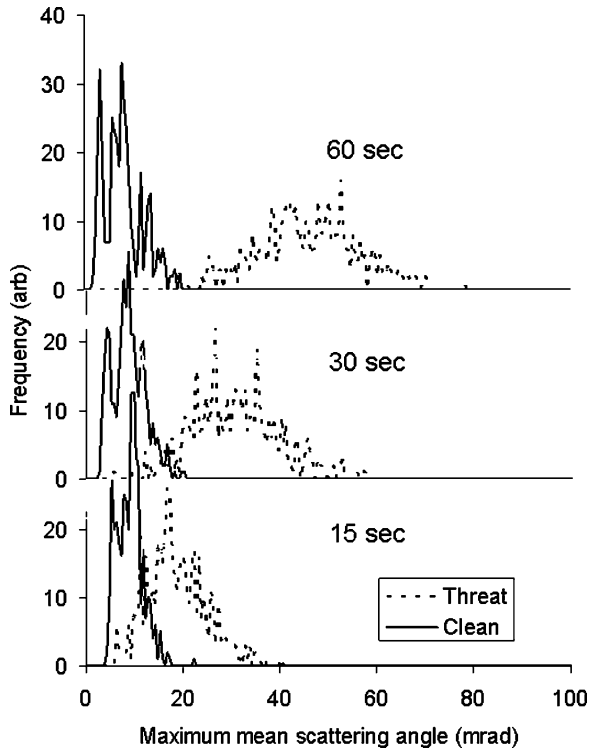


Figure 10: Same as Figure 9 but using prior knowledge as described in the text.

Singles rates in all of the tubes can be constantly monitored to provide gamma ray monitoring. The inner tubes can be filled with a gas mixture containing ^3He to provide neutron monitoring. In this case the neutron signals can be separated from gamma ray signals by their distinctive pulse height and shape.

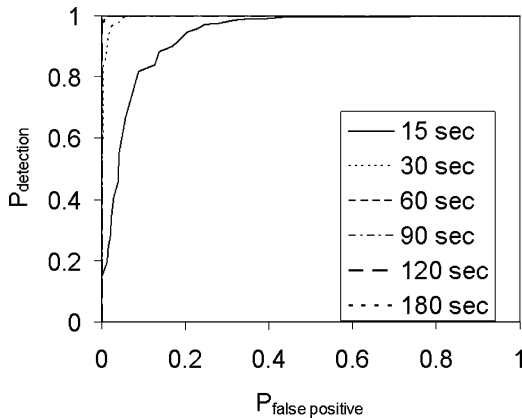


Figure 11: Same as Figure 8 except prior knowledge was used.

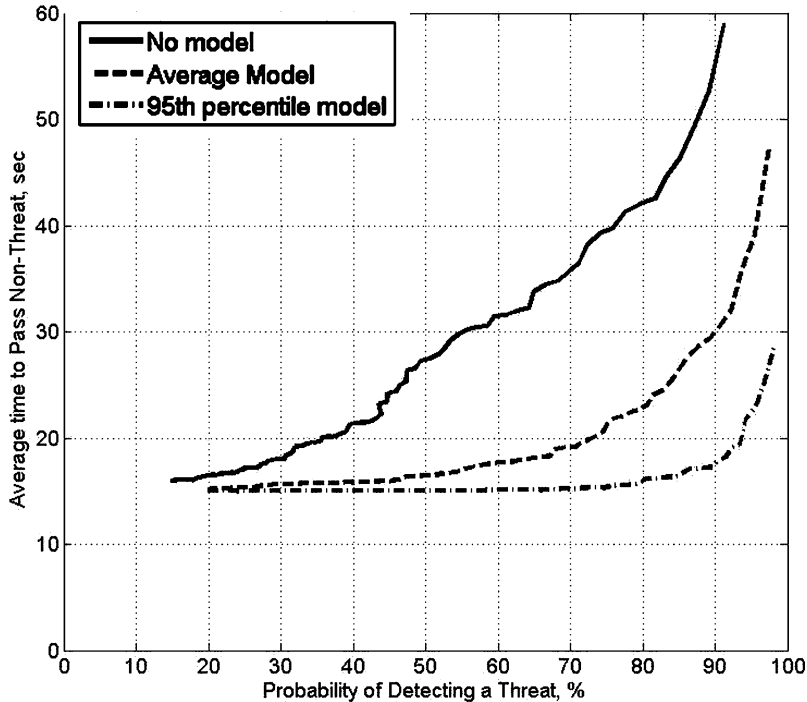


Figure 12: Comparison of average inspection times using no prior knowledge (solid line), straight subtraction (dash line), and three sigma subtraction (dot-dash line) for the mix of scenes described above.

Cost Estimates

A rough order of magnitude estimate of the cost of such a station can be obtained using estimates based on building large area detectors for high energy physics. An element of the detector might consist of a 5-cm-diameter aluminum tube with a small diameter ($20\ \mu\text{m}$) wire running down its axis.

The dominant costs of such detectors are in the readout and the mechanics at the end of the tubes. We estimate that the cost of a single coordinate measurement will be about \$200/cm, including both planes needed to fully reconstruct the drift time information. The cost of the six planes needed to measure both incoming and outgoing trajectories for an automobile-sized counting station, $4 \times 4 \times 5\ \text{m}^3$, would be about $\$3.0 \times 10^6$.

There are several differences between this application and a physics experiment. Cosmic ray counting rates are low when compared with most high-energy physics experiments. Consequently, one can reasonably expect long (decades) counter lifetimes. On the other hand, the large inexpensive skilled workforce required to maintain a high-energy detector will not be available at border crossings. Detectors will need to be low maintenance. We envision sealing the detectors to eliminate the need for flowing gas and maintenance of a gas system. The

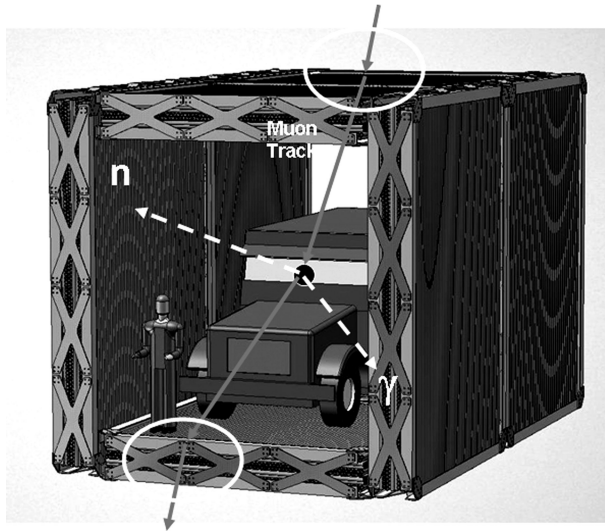


Figure 13: A schematic view of how a counting station might look. Vehicles would be stopped within the area covered by the counting station for a counting period ~ 20 s.

electronics need to be simple and robust and use a readily available commercial computer interface such as universal serial bus (USB). We have demonstrated that sealed drift tubes can meet the detector needs.

This technique enables examination of every vehicle and shipping container crossing the U.S. (or foreign) border. All that is needed is enough detectors at border crossings to handle the traffic. Using statistics compiled by the U.S. Department of Transportation for the year 2000,¹⁸ the total personal vehicle traffic crossing U.S.-Mexico and U.S.-Canada border was 1.3×10^8 . If a single muon tomography machine can analyze a vehicle within 1 min or less of counting/processing time, operating for 12 h per day, then only about 500 machines would be needed to handle the entire cross-border personal vehicle load. The total cost \$1.5 to 2 billion is negligible compared to the economic consequence of the detonation of a nuclear device within the U.S. borders. Queuing times and rate fluctuations may require quadrupling this estimate. A similar size effort would be need to handle commercial cross-border truck and seaport transportainers traffic.

The same technique can be used to examine cargo in trucks and transportainers. The long storage time of transportainers in transit in ships at sea suggests a possibility. Special transportainers containing position-sensitive detectors could be interspersed with normal cargo. Radiography could be accomplished using coincidence between these monitor transportainers to sample the cargo in the hold of the ship. Although this technique would not afford 100% coverage, it could take advantage of the transport time to survey some of the cargo in a ship.

CONCLUSION

We have described a technique for radiographing large objects with cosmic rays. This technique is particularly sensitive to high-Z dense materials. We have performed a considerable amount of experimental (LMT) and theoretical (GEANT/MLEM) analysis on automatically identifying 1000 cm³ nuclear threat objects in complicated background scenes. We have demonstrated detection times of ~4 min for data taken in an experiment. We expect on the order of a factor of 10 reduction in scanning times when we implement full solid angle scanning and momentum estimation, a factor of 2 from momentum estimation, and 5 from solid angle.

We have also estimated the times needed in larger and more complicated scenes using GEANT simulations and MLEM reconstructions. These assume the full solid angle, 50% momentum knowledge, and take advantage of fully three-dimensional density reconstructions, which reduce the noise levels. These demonstrate that by using prior knowledge, 17 s time scans provide >90% confidence identification of 1000-cm³ volumes of high Z material with less than 0.2% false-positive rates for the scenes studied.

It is possible that a perpetrator would seek to smuggle bomb components across the border in smaller packages than the 1000 cm³ corresponding to a mass of about 20 kilograms that has been considered here or in materials of less density. And, naturally, they could try to avoid any monitored crossing point altogether. Such possibilities would have to be considered in any overall assessment of our muon imaging concept along with other detection technologies.

In operation it is reasonable to expect 15-s scan times for occupied vehicle traffic. We have not studied cargo containers with our new, more sensitive techniques. Our previous work suggested that <60-s scanning times are feasible for a difficult mix of cargo containers loaded to their weight limit. With ML/EM there is every reason to expect these times to be shorter, but 60 s is a conservative estimate for cargo container scanning times.

A rough order of magnitude cost estimate for the capability of searching every incoming passenger vehicle of less than 1 billion dollars shows the technique to be economically viable.

We have also presented results from some studies that have used sealed drift tubes to study the potential for measuring gamma ray signals from nuclear threat objects. A full MT scanner should provide a gamma ray counting efficiency of >10% across a wide range of energies. Although not discussed above, gamma ray and neutron sources in a cargo volume can be localized using the position dependence of the signal. One conclusion is that RDD devices require enough radioactive material so that shielding them makes them highly visible in the MT images.

NOTES AND REFERENCES

1. F. Calogero, "Nuclear Terrorism." Speech given at the *Nobel Peace Prize Centennial Symposium: "The Conflicts of the 20th Century and the Solutions for the 21st Century,"* Session 6, "Militarism and Arms Races—Stengthen Arms Control and Disarmament" (Oslo, Norway, December 6–8, 2001).
2. E. R. Siciliano, J. H. Ely, R. T. Kouzes, B. D. Milbrath, J. E. Schweppe, and D. C. Stromswold, "Comparison of PVT and NaI(Tl) Scintillators for Vehicle Portal Monitor Applications," *Nuclear Instruments and Methods in Physics Research A*, 550 (2005), 3, 647–674.
3. J. I. Katz, G. S. Blanpied, K. N. Borozdin, and C. L. Morris, "X-Radiography of Cargo Containers," *Science & Global Security*, 15 (2007), 49–56.
4. K. N. Borozdin, G. E. Hogan, C. L. Morris, W. C. Friedhorsky, A. Saunders, L. J. Shultz, and M. E. Teasdale, "Radiographic Imaging with Natural Muons," *Nature*, 422 (2003), 277.
5. Particle Data Group. "Review of Particle Physics," *Physics Letters*, B592 (2004), 1.
6. W. Roentgen, "On a New Kind of Rays," *Nature*, 53 (1896), 274.
7. A. Beer, *Ann. Physik Chem.*, 86 (1852), 78.
8. N. King, E. Able, K. Adams, K. R. Alrick, J. F. Amann, S. Balzar, et al., "An 800-MeV Proton Radiography Facility for Dynamic Experiments," *Nuclear Instruments and Methods in Physics Research A*, 424 (1999), 84–91.
9. C. Morris, J. W. Hopson, and P. Goldstone, "Proton Radiography," *Los Alamos Science*, 30 (2006), 32–44.
10. B. Rossi, *High-Energy Particles* (Englewood Cliffs, NJ, Prentice-Hall, Inc., 1952).
11. S. Agostinelliae, J. Allison, K. Amakoe, J. Apostolakisa et al., "Geant4—A Simulation Toolkit," *Nuclear Instruments and Methods in Physics Research A*, 506 (2003), 250–303; "Geant4 Developments and Applications," *IEEE Transactions on Nuclear Science*, 53 (2006), 270–278.
12. J. A. Green, C. Alexander, T. Asaki, J. Bacon, G. Blanpied, K. Borozdin et al., "Optimizing the Tracking Efficiency for Cosmic Ray Muon Tomography," *2006 IEEE Nuclear Science Symposium Conference Record* (San Diego, CA, 2006).
13. G. E. Hogan, "PC DAQ, a Personal Computer Based Data Acquisition System," Los Alamos National Laboratory Report #LAUR-98-4531 (1998).
14. S. Fetter, V. A. Frolov, M. Miller, R. Mozley, O. F. Prilutskii, S. Rodionov, and R. Z. Sagdeev, "Detecting Nuclear Warheads," *Science and Global Security*, 1 (1990), 225–302.
15. K. J. Shultis and R. E. Faw, *Fundamentals of Nuclear Science and Engineering* (Boca Raton, FL, CRC Press, 2002).
16. L. J. Schultz, *Cosmic Ray Muon Tomography*, Ph.D. dissertation (Portland, OR: Portland State University, 2003).
17. L. J. Schultz, G. S. Blanpied, K. N. Borozdin, A. M. Fraser, N. W. Hengartner, A. V. Klimenko, C. L. Morris, C. Orum, and M. J. Sossong, "Statistical Reconstruction for Cosmic Ray Muon Tomography," *IEEE Transactions on Image Processing*, accepted (2007).
18. Bureau of Transportation Statistics, special tabulation. Based on the following primary data source: U.S. Department of Treasury, U.S. Customs Service, Office of Field Operations, Operations Management Database (Washington, DC: 2000), <http://www.bts.gov/> (accessed: December 12, 2001).